GEM TN-93-279
MIT-GEM-EM-014

Joule Heating of GEM Detector Bobbins

A. Radovinsky
Plasma Fusion Center, Massachusetts Institute of Technology

December 16, 1992

Abstract:

A study of Joule heating of GEM detector magnet bobbins has been carried out using the program EDDYCUFF. The results show that maximal Joule heating occurs in the peripheral bobbins walls during the discharge of the magnet. To reduce the heating a segmented bobbin design is suggested.

MIT-GEM-EM-014

Joule Heating of GEM Detector Bobbins

16 December 1992

A. Radovinsky

This document and all reports and memoranda in this series are intended as a record of work in progress. They are for use in informal discussions of design and fabrication alternatives. This material is subject to change and should not, therefore, be published or referred to in the open literature. Conclusions are preliminary and distribution should be strictly limited.

Plasma Fusion Center
Massachusetts Institute of Technology
Cambridge, MA 02139

MIT GEM Detector Memoranda
Approval Sheet

B.A. Smith
Project Engineer

12/17/92
Date

R.D. Pillsbury, Jr.
Technical Monitor

12/10/92
Date

for A.M. Dawson
A.M. Dawson
Technical Editor

16 Dec 1992
Date

SUMMARY

A study of Joule heating of GEM detector magnet bobbins has been carried out. The results are presented in this memo.

ANALYSIS

The program EDDYCUFF[1] was used in these analyses. EDDYCUFF assumes that the conducting medium is a shell which is thin relative to the skin depth, which implies a uniform distribution of current density through the thickness of the material. This also implies that there is no current flow perpendicular to the plane of the shell. The dimensions of the model are shown in Fig 1. An axial cross section of a set of 12 cylindrical coil modules and thin conducting bobbins is shown, with axial symmetry about the Z-axis and a plane of symmetry at Z=0.

The coils were modeled as uniform current density solenoids with a centroid radius of 9.5 m, thickness of 0.02 m, and length in Z-direction of 0.9709 m. The current (I) in all solenoids is the same.

The bobbin walls were modeled as cylindrical shells, with a centroid radius of 9.582 m, thickness of 0.076 m, and length in the Z-direction of 1.1875 m. For cases in which the bobbin walls were modeled with flanges (see Fig 2), an additional thickness, equivalent to the cross section of a flange (0.026 m^2), was added to the elements of the bobbin at each end of the bobbin section.

The thermal radiation intercepts were modeled as cylindrical shells with a centroidal radius of 9.453 m, thickness of 0.0064 m, and length in the Z-direction of 1.1875 m.

The eddy currents and the Joule losses were calculated for bobbin walls or radiation intercepts of each bobbin separately (i.e. the effect of the eddy currents in one bobbin section on the eddy currents of other bobbin sections is ignored). Because of the symmetry of the design, the results are given for 12 bobbins, as shown in Fig 1.

The resistivity of the material of the bobbins was assumed to be $1.4*10^{-8}$ Ohm*m, which corresponds to Al 6061 at 4 K.

Two transient regimes were considered. They were:

* Charging the coil sections with a linear current ramp from 0 to 950 kA in 8 hours;

* Discharge, with an exponential current decay characterized by a time constant of 100 sec. That is

$$I=950*\exp(-t/100) \quad kA$$

A comparison of two designs was made: the design with bobbins made of continuous cylindrical shells, and the design with bobbins made up of four cylindrical segments (quadrants) electrically isolated from one another.

Five cases were considered

A. Charging of continuous bobbin walls without flanges;

B. Charging of segmented bobbin walls without flanges;

C. Discharge of segmented bobbin walls without flanges;

D. Discharge of segmented bobbin walls with flanges;

E. Discharge of segmented radiation intercepts.

RESULTS

The results of the study are summarized in Table 1 which shows the values of the thermal energy (in Joules) generated in each of the bobbin sections. Table 2 shows the peak values of the generated power (in Watts). In the cases of charging (A, B) the power deposition is uniform during all 8 hours of the ramp. During discharge, it has a peak at 5, 9, and 1 sec. for cases C, D, and E respectively. Fig 3 shows the discharge curves for cases C and D. The values shown in Table 1 for the cases C, D, and E account for about 98% of the actual energy of discharge, since they were obtained by numerical integration of the Joule heating power during only the first 200 seconds.

The distribution of the losses among the bobbins depends primarily on whether the bobbins are continuous or segmented. The distributions are shown on Figs 4a and 4b for cases A and B, i.e. for charging of continuous and segmented bobbins, respectively. In cases C, D, and E, runs for only the 12-th bobbin were made, and results for other bobbins were scaled by the distribution calculated for all bobbins in case B. A check of this scaling in the eleventh bobbin (second highest loss) showed an accuracy within 2% of the calculated value.

Comparison of the data of Tables 1 and 2 shows the following:

* The design with continuous elements (case A) will have 3080 times the losses of the split design (case B).

* In the cases of segmented bobbins (cases B-E) the highest heating occurs in the 12-th bobbin which comprises about 48% of the heating of all the 12 bobbins.

* In the cases of segmented bobbin walls (w/o flanges) the peak power generated during dischage (case C) is about 75000 times higher than that during charge (case B), and the ratio of the heating energy for these two cases is 140.

* The design with flanges electrically connected to the bobbin walls (case D) compared to that without flanges (case C) shows 2.34 times higher values of energy and peak power.

* Losses in the radiation intercept (case E) are substantionaly lower than in any of the designs of the bobbin walls considered in this study.

To verify these results, a test run using MITMAP[2] was made for case A and results (Joule losses) were compared to the results for the EDDYCUFF program. Comparison showed less than a 1% difference. Also, analytic estimates using equations[3] similar to those on which EDDYCUFF is based in quasi-static (resistive) approximation were made for both charge and discharge regimes for the design with quadrants (cases B and C). These estimates (in case C - for time points after the peak) showed the same difference in the Joule losses compared to the numeric results by EDDYCUFF. In both cases the analytical results are 66% higher than those obtained numerically. This error can be explained by the inaccuracy of the analytical approximation of the driving B-field on the surface of the bobbin assumed in the analytic estimates.

Figs 5a -5e show the distribution of eddy currents in the 1/8-th segment of the elements of the 12-th bobbin (see Fig 1) for the corresponding cases.

---

[1] *EDDYCUFF User's Manual ... (To be published)*

[2] *Robert D.Pillsbury, Jr., MAP User's Manual, PFC/RR-91-5, December 1991, MIT Plasma Fusion Center, Cambridge, MA 02139*

[3] *A.L.Radovinski,"On the equations of electromagnetic processes in electrically conducting shells," Soviet Power Engineering, no.4, 1987.*

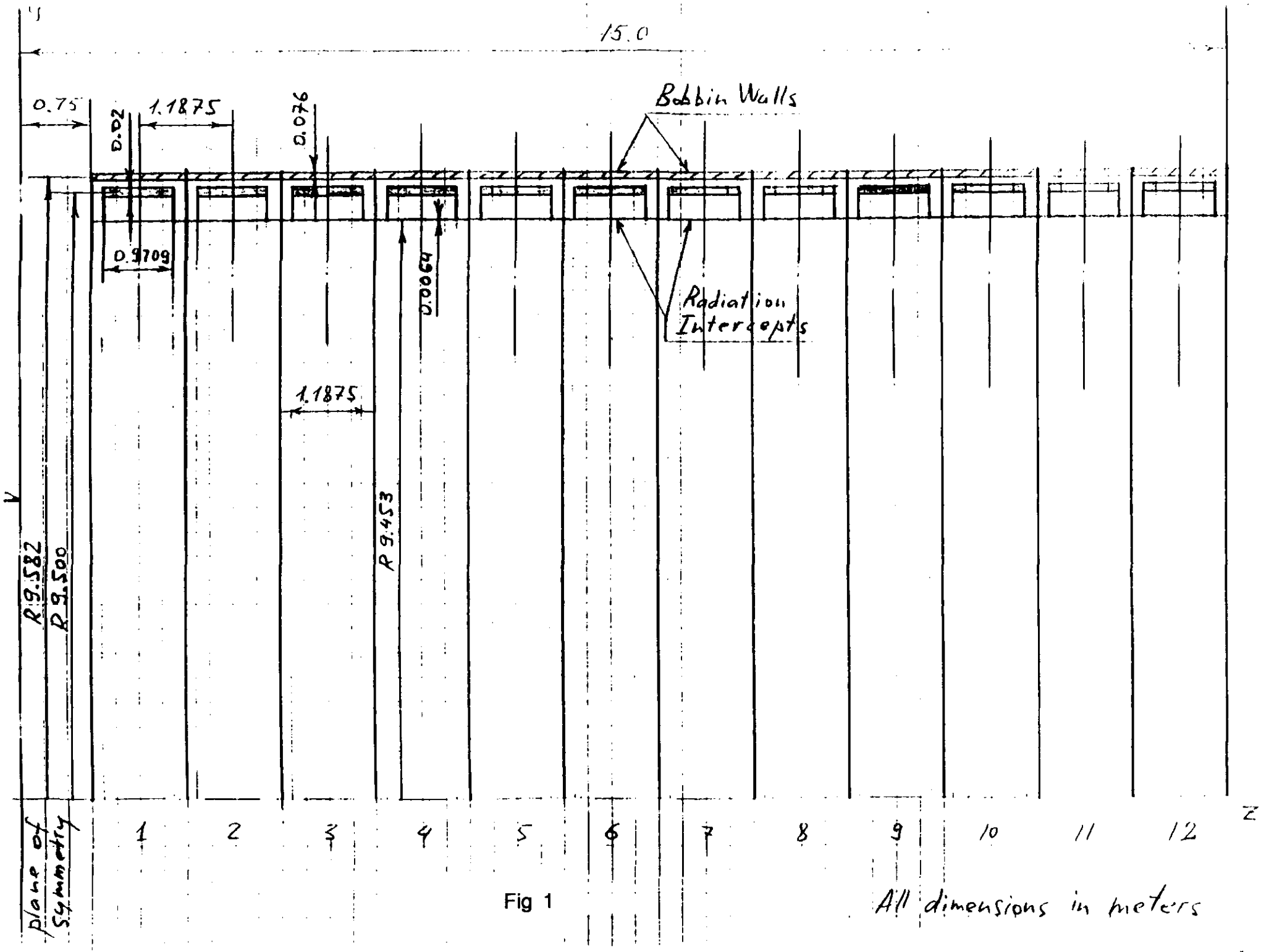
15.0
0.75
1.1875
0.02
0.076
Bobbin Walls
0.9709
0.0064
Radiation Intercepts
1.1875
R 9.582
R 9.500
R 9.453
Y
Z
plane of symmetry
1
2
3
4
5
6
7
8
9
10
11
12
All dimensions in meters

Fig 1

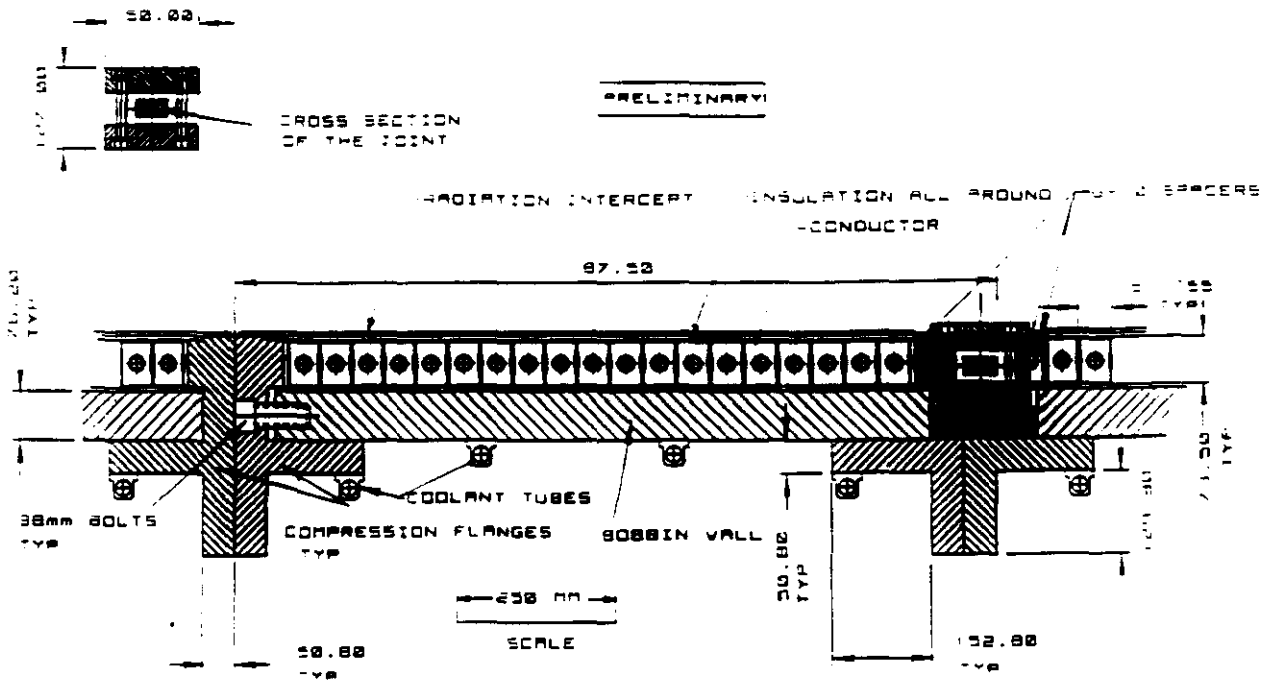

Fig 2. Coil Model Cross Section

Thermal Energy (J)																
Bobbin no.	>>>	>>>	>>>	1	2	3	4	5	6	7	8	9	10	11	12	all 12
Element	Description	Regime	Case													
Bob. wall	Cont. w/o fl.	Charge	A	177790	190777	195515	196595	194359	189757	182154	171966	158221	140829	118197	87902	2004063
Bob. wall	Quadr. w/o fl.	Charge	B	57	11	5	5	6	8	13	21	35	60	115	316	652
Bob. wall	Quadr. w/o fl.	Discharge	C	7958	1573	766	661	820	1184	1845	2921	4836	8348	16127	44221	91260
Bob. wall	Quadr. w. fl.	Discharge	D	18623	3681	1793	1547	1918	2770	4318	6836	11318	19536	37741	103488	213569
Rad. interc	Quadr.	Discharge	E	681	135	66	57	70	101	158	250	414	715	1381	3787	7815

Table 1. Summary of Thermal Energy Generated in Bobbin Elements

Max. Power (W)																	
Bobbin no.	>>>	>>>	>>>	>>>	1	2	3	4	5	6	7	8	9	10	11	12	all 12
Element	Description	Regime	Case	Time													
Bob. wall	Cont. w/o fl.	Charge	A	All	6.17	6.62	6.79	6.83	6.75	6.59	6.32	5.97	5.49	4.89	4.10	3.05	69.59
Bob. wall	Quadr. w/o fl.	Charge	B	All	0.0020	0.0004	0.0002	0.0002	0.0002	0.0003	0.0005	0.0007	0.0012	0.0021	0.0040	0.0110	0 0226
Bob. wall	Quadr. w/o fl.	Discharge	C	5 s.	148,7	29.4	14.4	12.4	15.4	22.2	34.5	54.6	90.4	155.9	301.2	825.9	1705.0
Bob. wall	Quadr. w. fl.	Discharge	D	9 s.	325.6	64.5	31.5	27.2	33.6	48.5	75.6	119.5	197.8	341.4	659.4	1808.0	3732.7
Rad. interc	Quadr.	Discharge	E	1 s.	13.76	2.72	1.33	1.15	1.42	2.05	3.19	5.05	8.36	14.42	27.86	76.38	157.70

Table 2. Summary of Peak Power Generated in Bobbin Elements

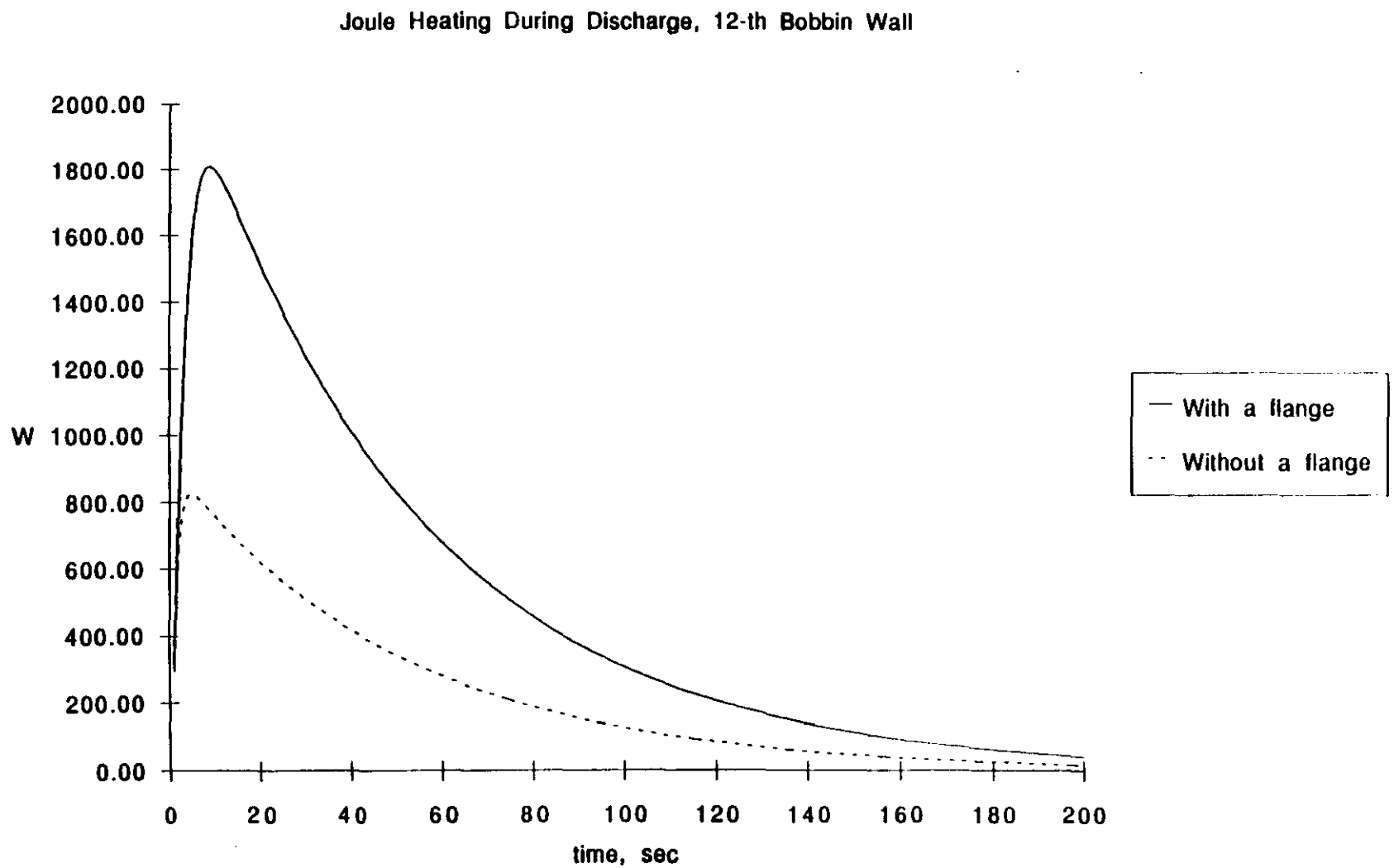
Joule Heating During Discharge, 12-th Bobbin Wall
2000.00
1800.00
1600.00
1400.00
1200.00
W 1000.00
800.00
600.00
400.00
200.00
0.00
0
20
40
60
80
100
120
140
160
180
200
time, sec
With a flange
Without a flange

Fig 3

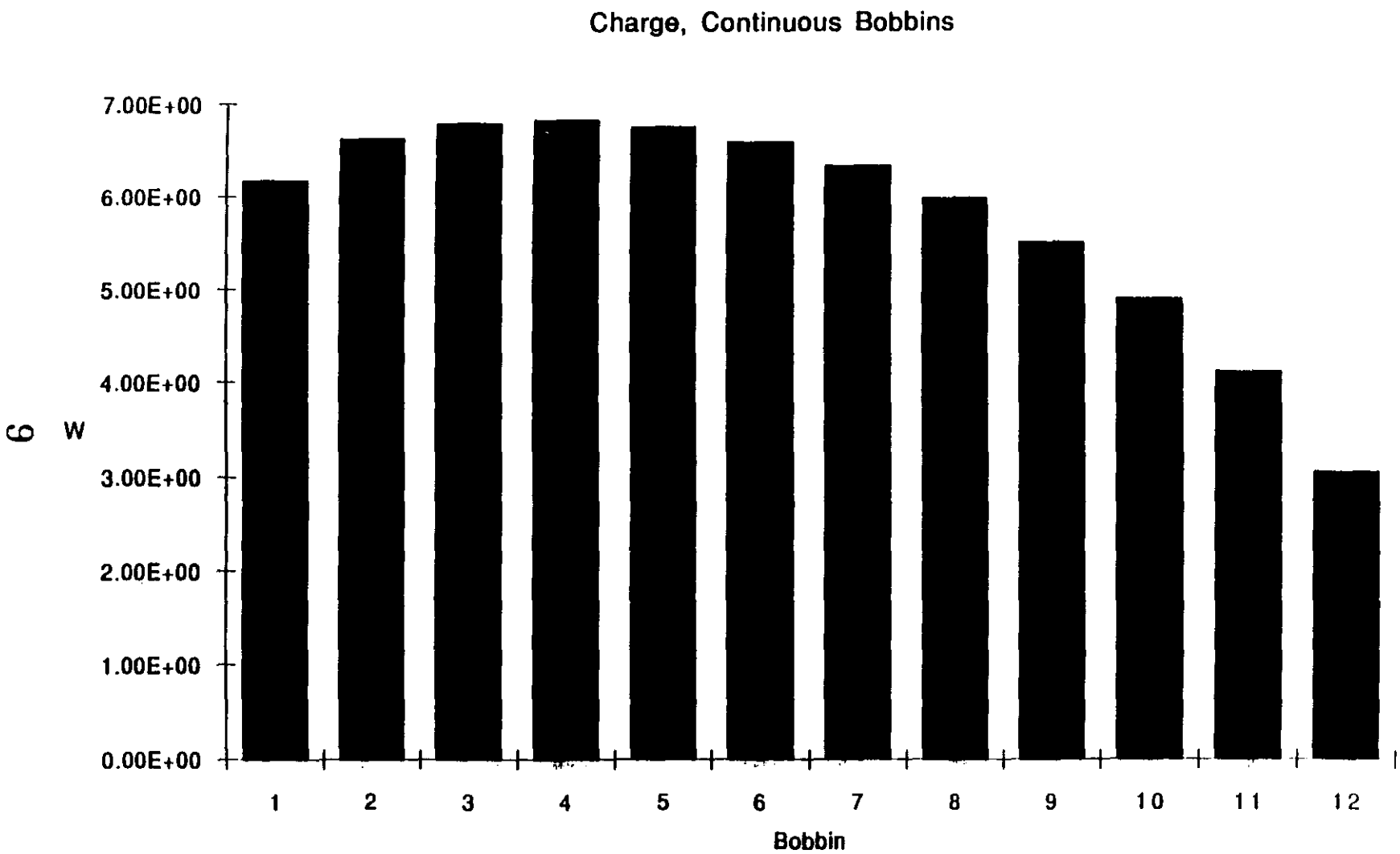
Charge, Continuous Bobbins
7.00E+00
6.00E+00
5.00E+00
4.00E+00
3.00E+00
2.00E+00
1.00E+00
0.00E+00
W
1
2
3
4
5
6
7
8
9
10
11
12
Bobbin

Fig 4 a

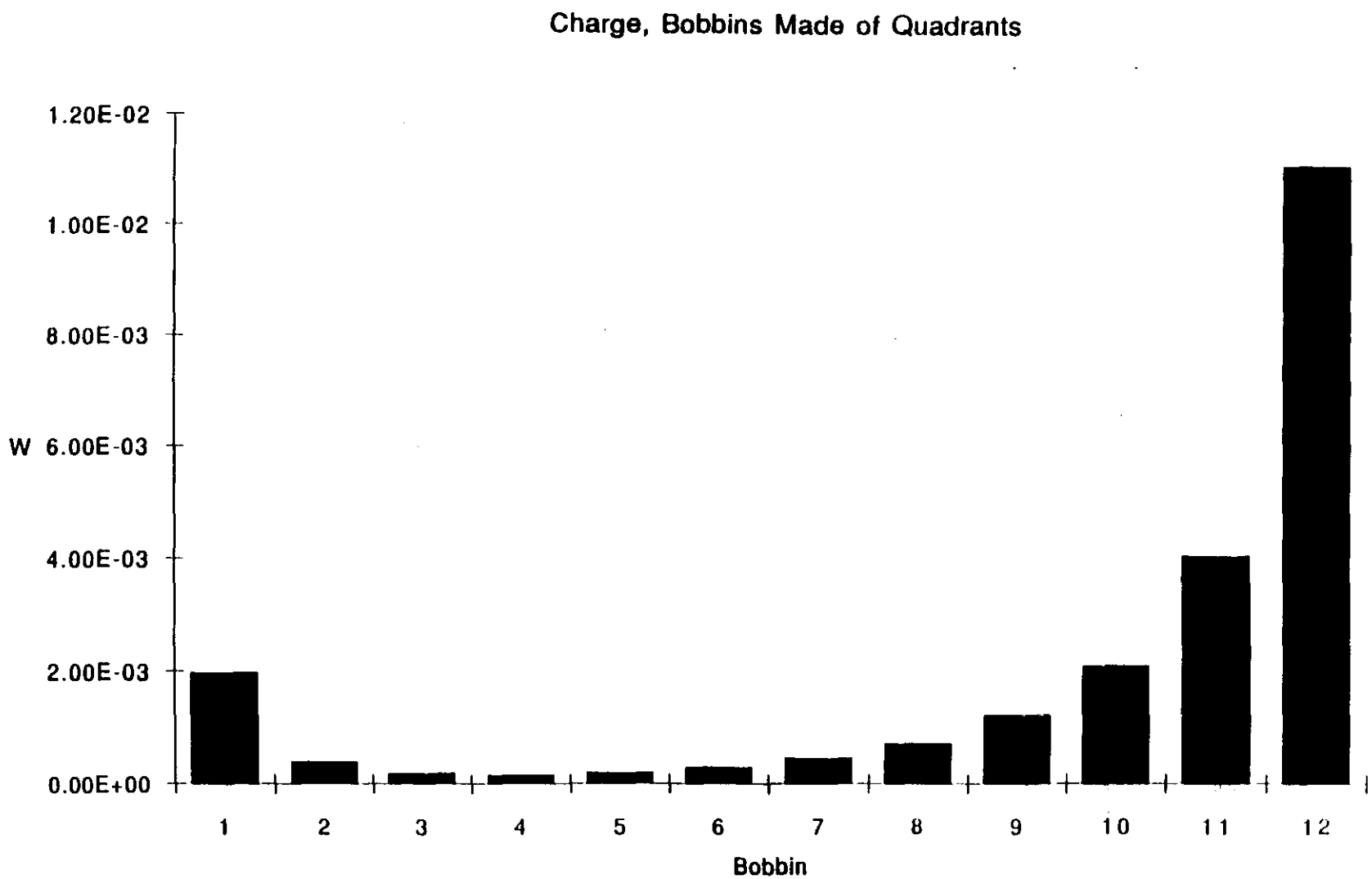
Charge, Bobbins Made of Quadrants
1.20E-02
1.00E-02
8.00E-03
W 6.00E-03
4.00E-03
2.00E-03
0.00E+00
1
2
3
4
5
6
7
8
9
10
11
12
Bobbin

Fig 4 b

Fig 5a Distribution of Current Density During Charge in One Half of the 12-th Bobbin Quadrant (w/o Flanges) where the Bobbins are Azimuthally Continuous (case A)

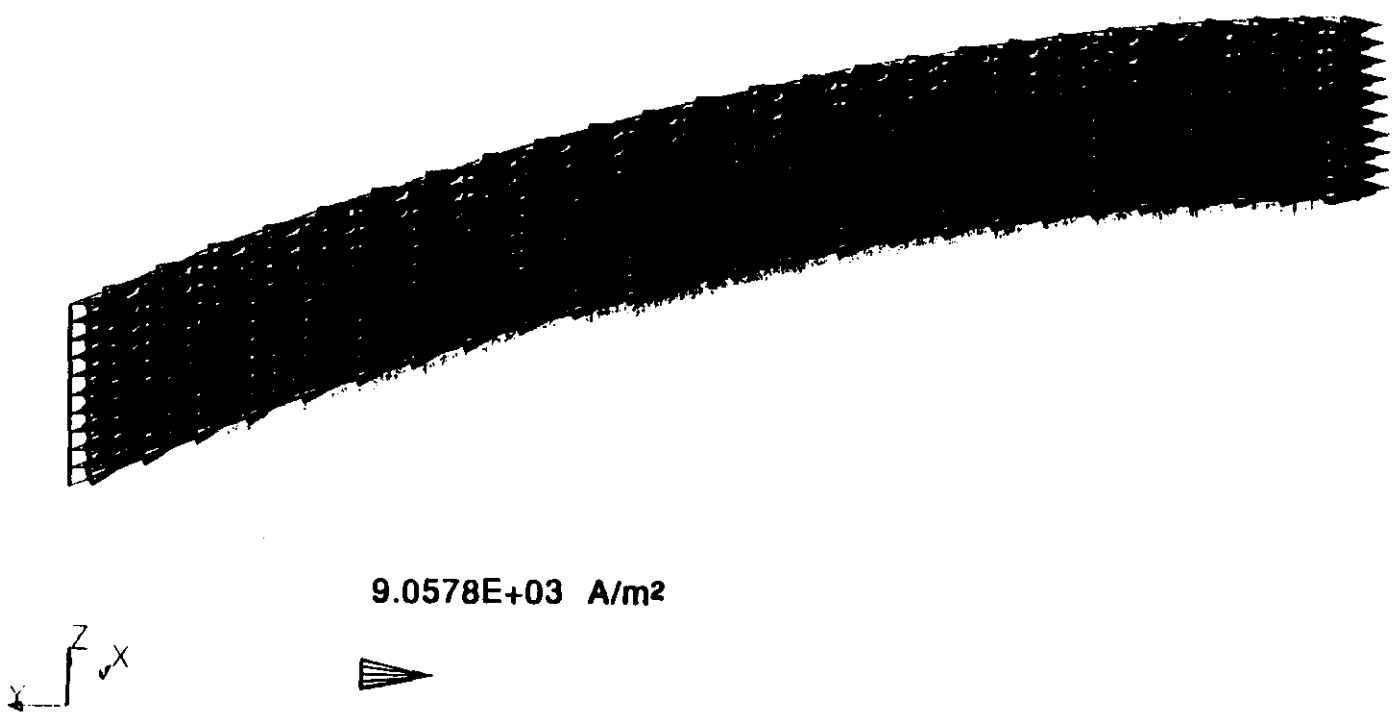

Fig 5b Distribution of Current Density During Charge in One Half of the 12-th Bobbin Quadrant (w/o Flanges) where the Bobbins are Azimuthally Discontinuous (case B)

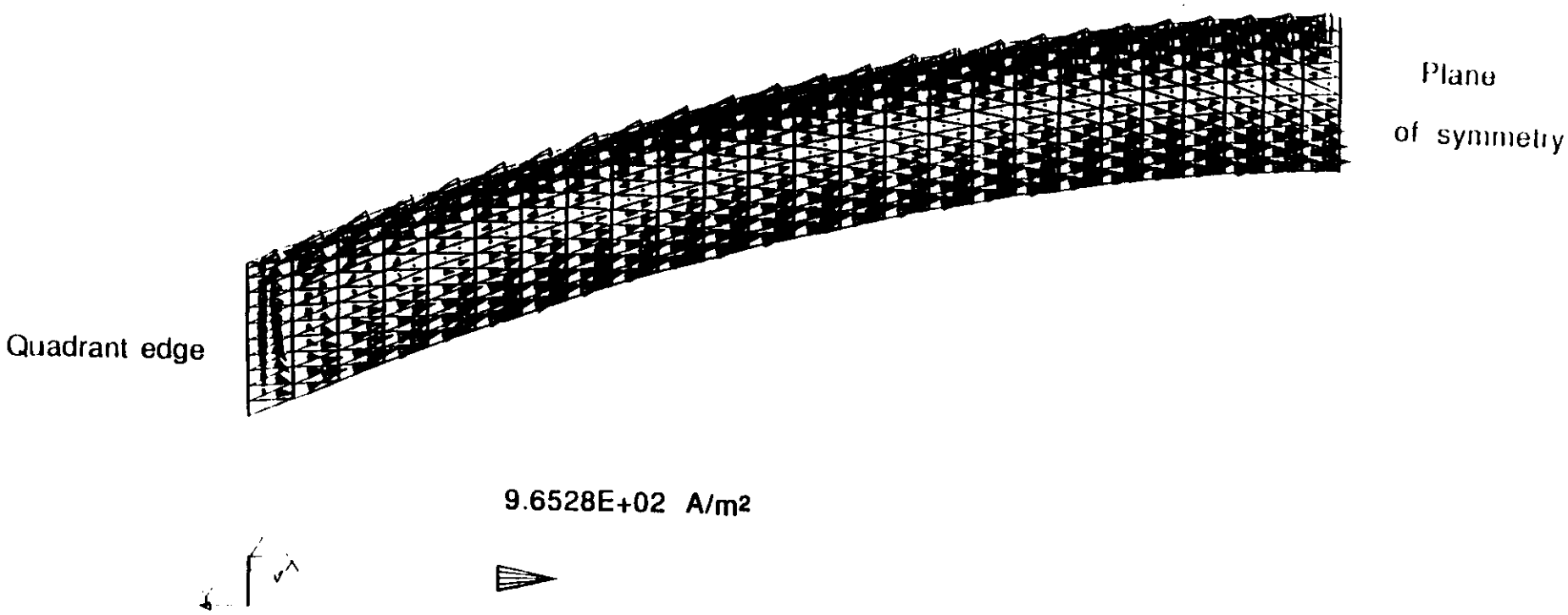

Fig 5c Distribution of Current Density During Discharge in One Half of the 12-th Bobbin Quadrant (w/o Flanges) where the Bobbins are Azimuthally Discontinuous (case C)

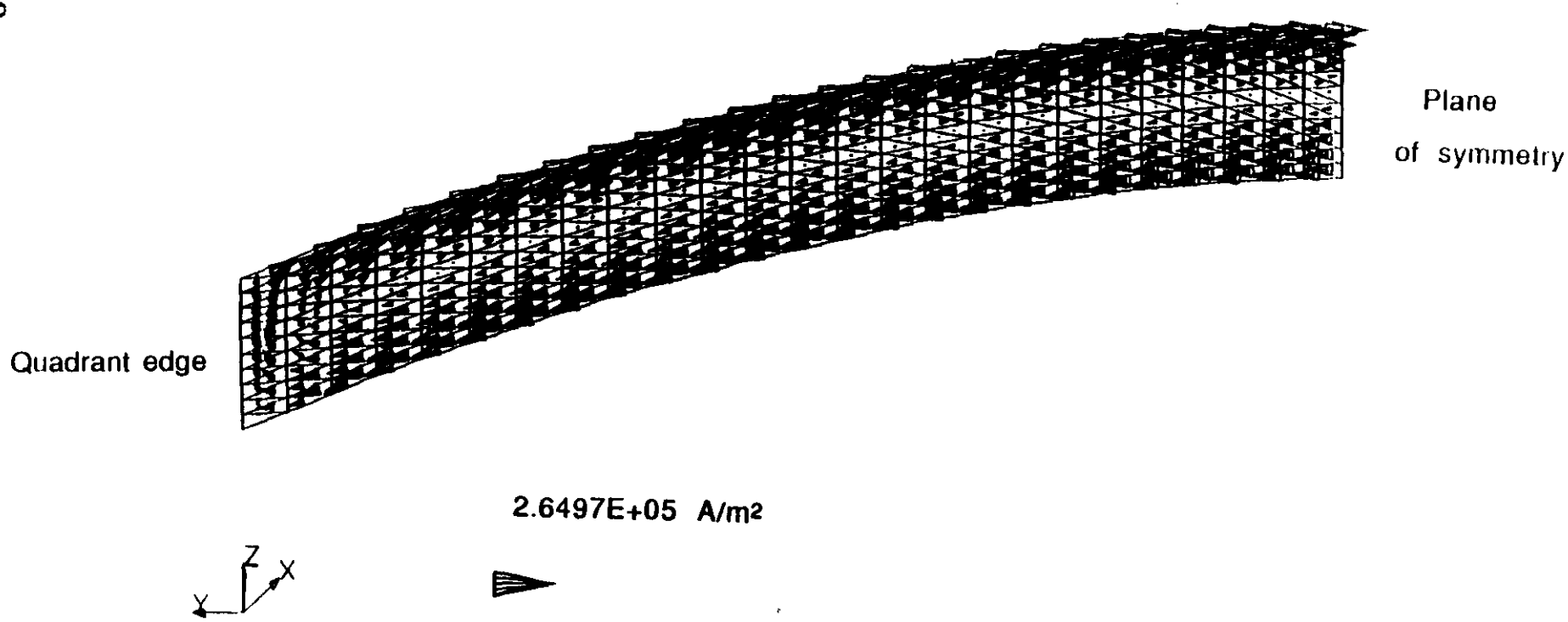

Fig 5d Distribution of Current Density During Discharge in One Half of the 12-th Bobbin Quadrant (with Flanges) where the Bobbins are Azimuthally Discontinuous (case D)

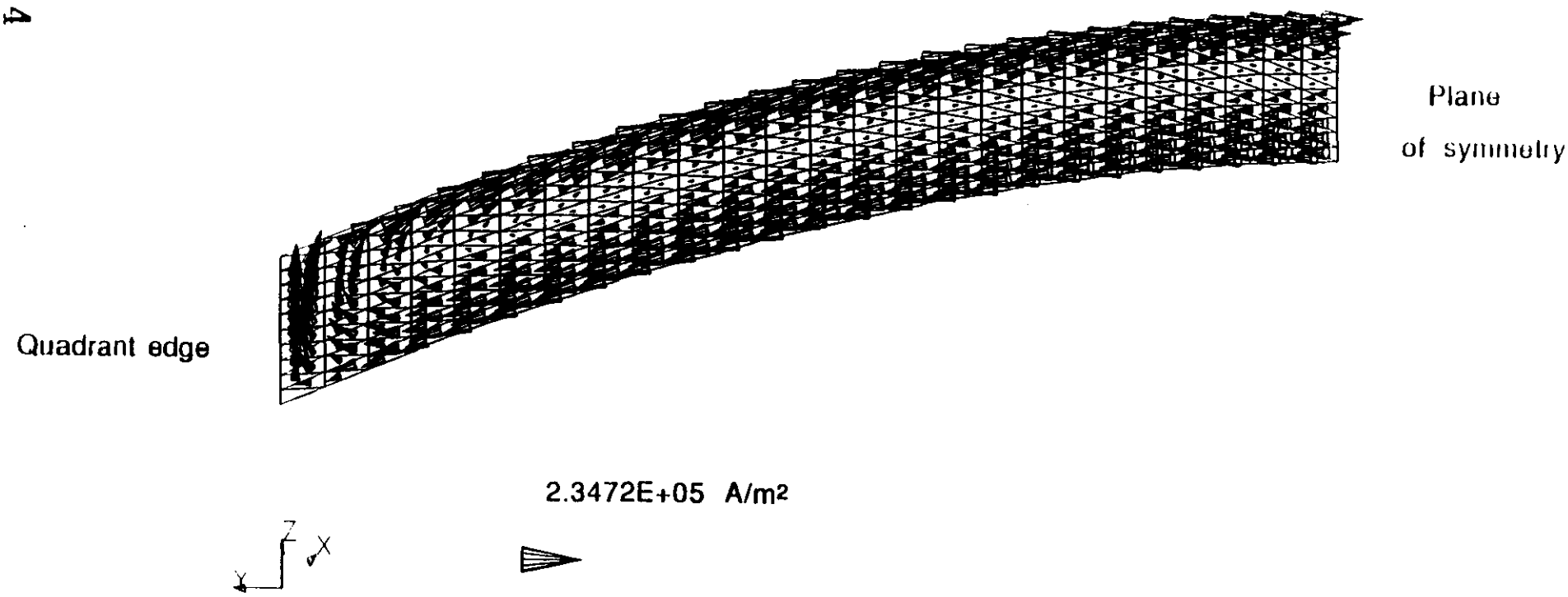
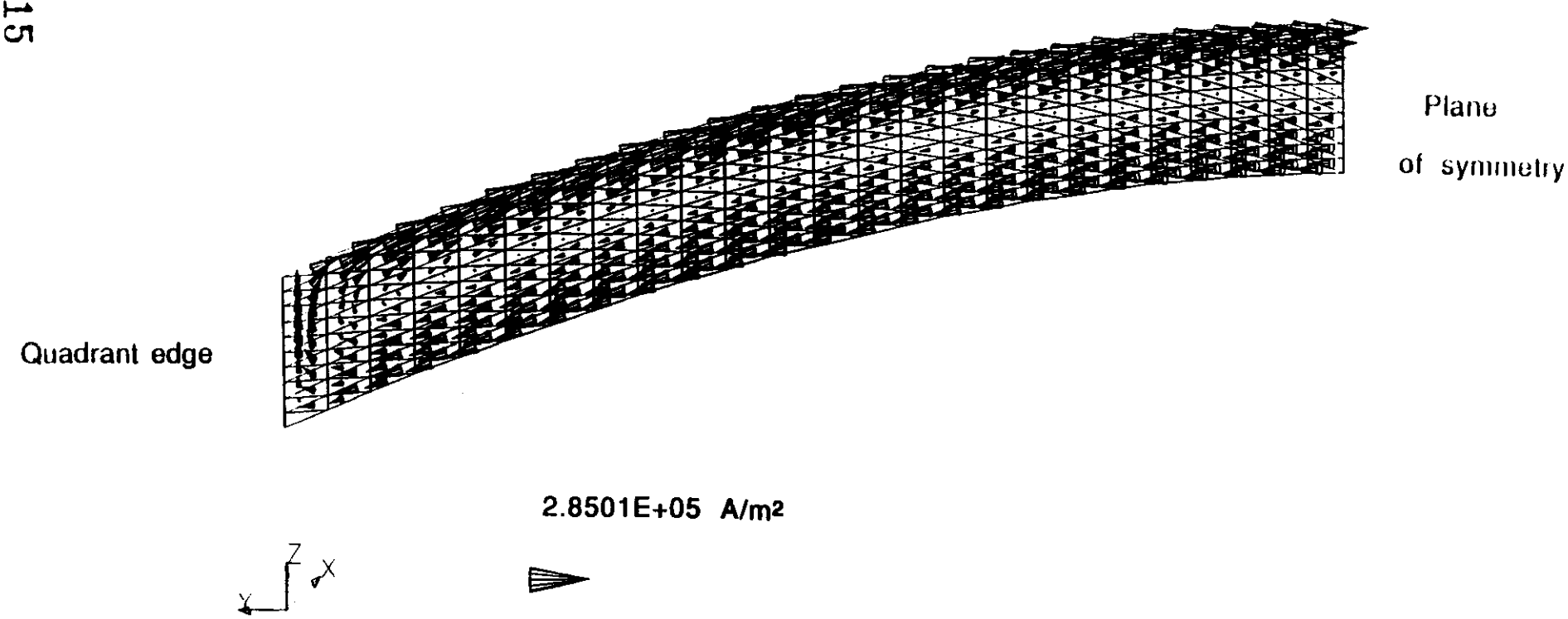
Fig 5e Distribution of Current Density During Discharge in One Half of the 12-th Bobbin Radiation Intercept Quadrant where the Intercepts are Azimuthally Discontinuous (case E)